

Variation of the Electrochemical Transfer Coefficient with Potential

BY JEAN-MICHEL SAVÉANT AND DIDIER TESSIER

Laboratoire d'Electrochimie de l'Université de Paris 7,
2 Place Jussieu, 75251 Paris Cedex 05, France

Received 14th May, 1982

The electrochemical electron-transfer rate constant has been determined as a function of the electrode potential for a series of simple electron-transfer processes to organic molecules in media containing acetonitrile or dimethylformamide and a quaternary ammonium salt as supporting electrolyte and using mercury as the electrode material. The reactions and the experimental conditions were selected so as to deal with outer-sphere processes and to minimize the magnitude of double-layer corrections. Convolution potential-sweep voltammetry and the impedance method were used for obtaining the kinetic data. Under these conditions, the electrochemical transfer coefficient was observed, in all cases, to vary, beyond experimental error, with the electrode potential. The magnitude of the variation is of the same order of magnitude as that predicted by the Marcus theory of outer-sphere electron transfer. A more complex reaction, the reduction of benzaldehyde in ethanol, involving dimerization steps following the initial electron transfer was also investigated. A definite variation of the transfer coefficient was again observed. This behaviour, observed for various solvents and functional groups, appears as a general phenomenon in the reduction of organic molecules in the case where charge transfer is fast and mainly governed by solvent reorganization.

The present theories of electron transfer at electrodes,¹ such as the Hush–Marcus theory,^{2–4} predict that the electrochemical transfer coefficient should vary with the electrode potential. Being based on an harmonic approximation they imply a quadratic dependence of the activation energy and therefore a linear dependence of the electrochemical transfer coefficient upon the electrode potential. They also predict the magnitude of the variation of the transfer coefficient as a function of the reorganization factor. The smaller the reorganization factor, *i.e.* the faster the electron transfer, the larger the variation of the transfer coefficient with potential.

Over the last 15 years there have been several attempts to detect such variations experimentally and to compare their magnitude with that anticipated from the theory.^{5–19} Earlier work^{5–11} in this area has not provided a clear answer to the question thus raised. The same systems that were first regarded as exhibiting such a potential dependence⁵ were later, after more accurate analysis, shown not to give rise to a definite variation that was clearly greater than experimental error.⁷ In order to obtain acceptable evidence that the transfer coefficient does or does not vary with the potential, the system under study must fulfil several requirements. The first of these is that the electrochemical reaction should follow a simple mechanism, preferably involving a single one-electron step giving rise to a chemically stable species, at least in the time range of the experiments. This does not mean that it is impossible to investigate the potential dependence of the transfer coefficient in more complex processes, involving for example follow-up chemical steps. However, it appears safer to start with elementary electron-transfer processes. When going to systems involving associated chemical reactions, the nature of these chemical steps should be ascertained and their occurrence be under proper experimental control. It is also required that the electron transfer be an outer-sphere process with no concomitant bond breaking

or bond formation. Similarly, adsorption of reactants on the electrode surface should be avoided. Since double-layer effects can interfere with the apparent variation of the transfer coefficient with potential, it is important that the structure of the electrode–electrolyte interface be properly defined. In this connection, it is preferable to use mercury as the electrode material rather than solid electrodes. The influence of double-layer effects increases with the charge of the reactants. Since corrections of the double-layer effects are sources of uncertainty, $+1/0$ or $0/-1$ couples are expected to be the most useful.

In order to obtain the maximum accuracy in the detection of variations of the transfer coefficient, the potential range where the kinetic determinations are carried out should be as large as possible. Within a given time-scale the available potential range increases as the rate of electron transfer decreases. However, the variations of the transfer coefficient decrease as the rate of electron transfer decreases. The investigation of very fast electron transfers is, however, limited by the necessity of going to very short time-scales in order for the system to depart from electrochemical reversibility. The kinetic determinations then become less and less accurate.

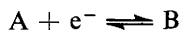
Of the reactions investigated with the aim of detecting the anticipated potential dependence of the transfer coefficient, the reduction of organic molecules giving rise to stable anion radicals in non-aqueous organic media, in the presence of quaternary ammonium salts on a mercury electrode, appears a good candidate for fulfilling the requirements discussed above. Quaternary ammonium cations are not specifically adsorbed on the mercury electrode surface in non-aqueous solvents such as acetonitrile²⁰ and DMF.²¹ The effect of the double layer on the electron-transfer kinetics can thus be estimated with reasonable accuracy using the Gouy–Chapman theory of the double layer in the absence of specific adsorption of the ions of the supporting electrolyte. Since the considered redox couple involves a neutral molecule and a mononegative species the double-layer effects are minimized. The use of an aprotic organic solvent also favours the chemical stability of anion radicals since attack by acids or electrophiles are minimized. There are a number of aromatic molecules that give rise to stable anion radicals under such conditions, provided the presence of good leaving groups such as halogens is avoided. The negative charge is then generally delocalized over a rather large volume leading to small solvation reorganization factors and hence to fast electron transfer.²² Mononitro derivatives such as nitrobenzene and nitromesitylene appear to be good choices for investigating slower electron-transfer processes with the ensuing advantage of more accuracy in rate determinations. A large portion of the negative charge in the anion radical is located on the nitro group, giving rise to larger solvation reorganization factors and thus slower electron transfer.²³ Aliphatic nitro compounds can also be investigated since the nitro group both facilitates the reduction and chemically stabilizes the anion radical.²³

In this paper we describe and discuss the results obtained from the reduction of organic molecules, including nitro compounds, on mercury in acetonitrile (ACN) and dimethylformamide (DMF) containing a tetra-alkylammonium salt as supporting electrolyte. These compounds give rise to a stable anion radical which allowed the investigation of an electrochemical reaction consisting of an outer-sphere electron transfer. The reduction of benzaldehyde in buffered ethanol will provide an example of a more complex electrochemical reaction where an initial outer-sphere electron-transfer step is followed by a dimerization reaction. Two different electrochemical techniques were employed for the rate determinations: convolution potential-sweep voltammetry (c.p.s.v.) and impedance measurements.

[View Online](#)

**THE PREDICTED POTENTIAL DEPENDENCE OF THE
ELECTROCHEMICAL TRANSFER COEFFICIENT**

Considering the electron transfer



z being the charge of A and $z - 1$ that of B, the rate law can be written as

$$\frac{i}{FS} = k(E) \left\{ (C_A)_0 - (C_B)_0 \exp \left[\frac{F}{RT} (E - E^\ominus) \right] \right\}$$

where i is the current, S the electrode surface area, $(C_A)_0$ and $(C_B)_0$ the reactant concentrations just outside the diffuse double layer, E the electrode potential, E^\ominus the standard potential of the A/B couple and $k(E)$ the potential-dependent rate constant of the forward electron transfer.

According to the Marcus theory,^{2,3} $k(E)$ depends quadratically upon the electrode potential according to

$$-\frac{RT}{F} \ln \frac{k(E)}{Z_{e1}} = z\varphi_r + \frac{\lambda_0}{4F} + \frac{E - E^\ominus - \varphi_r}{2} + \frac{F}{4\lambda_0} (E - E^\ominus - \varphi_r)^2$$

View Online

where λ_0 is the reorganization factor, Z_{e1} the heterogeneous collision frequency and φ_r the potential difference between the reaction site and the solution.

The apparent transfer coefficient as defined by

$$\alpha_{ap} = -\frac{RT}{F} \frac{\partial \ln k(E)}{\partial E} \quad (1)$$

is thus given by

$$\alpha_{ap} = z \frac{\partial \varphi_r}{\partial E} + \left(1 - \frac{\partial \varphi_r}{\partial E} \right) \left(0.5 + \frac{F}{2\lambda_0} (E - E^\ominus - \varphi_r) \right).$$

There are two ways of defining the transfer coefficient:

$$\bar{\alpha} = 0.5 + \frac{F}{2\lambda_0} (E - E^\ominus - \varphi_r)$$

$$\alpha = 0.5 + \frac{F}{4\lambda_0} (E - E^\ominus - \varphi_r)$$

$\bar{\alpha}$ and α are related by: $2\alpha = 0.5 + \bar{\alpha}$.

$$\bar{\alpha} = \left(\alpha_{ap} - z \frac{\partial \varphi_r}{\partial E} \right) / \left(1 - \frac{\partial \varphi_r}{\partial E} \right) \quad (2)$$

is readily derived from α_{ap} , which is obtained from the experimental plots of $\ln k(E)$ against E , while α is conveniently used for obtaining the reorganization factor λ_0 from the same plots, according to

$$k(E) = k_{s,ap} \exp \left(-\frac{\alpha F}{RT} (E - E^\ominus) \right)$$

with

$$k_{s,ap} = k_s \exp \left(\frac{(\alpha - z)F\varphi_r}{RT} \right) \text{ and } k_s = Z_{e1} \exp \left(-\frac{\lambda_0}{4RT} \right).$$

Comparison between the predicted and experimental variations of the transfer coefficient can be made using $\bar{\alpha}$ or α

$$\frac{\partial \bar{\alpha}}{\partial E} = \frac{F}{2\lambda_0} \left(1 - \frac{\partial \phi_r}{\partial E} \right), \quad \frac{\partial \alpha}{\partial E} = \frac{F}{4\lambda_0} \left(1 - \frac{\partial \phi_r}{\partial E} \right).$$

SIMPLE ELECTRON-TRANSFER REACTIONS

CONVOLUTION POTENTIAL-SWEEP VOLTAMMETRY

Convolution potential-sweep voltammetry (c.p.s.v.)^{24,25} is a procedure for treating the current-potential curves obtained from cyclic voltammetry (c.v.). The experimental current, i , is transformed by convolution with the linear diffusion characteristic function $(\pi t)^{-\frac{1}{2}}$ into a "convoluted" current, I :

$$I = \frac{1}{\pi^{\frac{1}{2}}} \int_0^t \frac{i(\eta)}{(t-\eta)^{\frac{1}{2}}} d\eta.$$

The convoluted current is then used jointly with the current itself to determine the forward rate constant $k(E)$ as a function of the electrode potential according to: [View Online](#)

$$\log k(E) = \log(D_A \lambda^{\frac{1}{2}}) - \log \frac{I_1 - I \left[1 + \exp\left(\frac{F}{RT}(E - E^\ominus)\right) \right]}{i} \quad (3)$$

where D_A is the diffusion coefficient of the reactant, I_1 the plateau value of I , assuming that the reversible half-wave potential and the standard potential of the A/B couple are practically the same. Fig. 1 gives an example of a cyclic voltammetric curve and of the corresponding convolution potential-sweep curve for t-nitrobutane in DMF + 0.1 mol dm⁻³ Bu₄NI. This also illustrates a convenient way of determining the standard potential of the A/B couple, based on the determination of the potential,

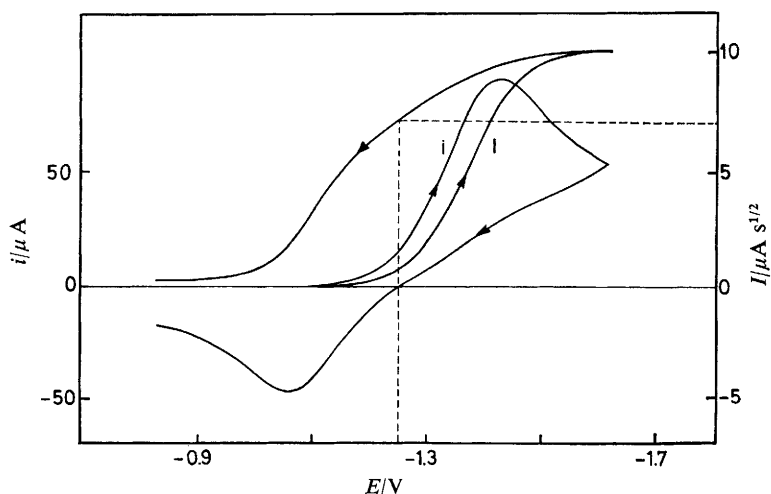


FIG. 1.—Cyclic voltammetry and convolution potential-sweep voltammetry of t-nitrobutane in DMF + 0.1 mol dm⁻³ Bu₄NI. Concentration, 1.5 mmol dm⁻³; sweep rate, 17.9 V s⁻¹. E is referred to the Ag, AgI electrode.

$E_{i=0}$, where the backward c.v. current intersects the potential axis, using the relationship:

$$E^\ominus = E_{i=0} - \frac{RT}{F} \ln \left(\frac{I_1 - I_{i=0}}{I_{i=0}} \right).$$

C.p.s.v. presents two advantages over the conventional use of cyclic voltammetric peak separation. The first of these is that the form of the rate law, $k(E)$, need not be *a priori* specified for treating the data. The second is that all the information contained in the voltammetric curve is used instead of only that provided by the c.v. peaks.

Fig. 2(a) shows plots of $k(E)$ against E obtained by these procedures for t-nitrobutane in ACN and DMF, and for nitrodurene and nitromesitylene in ACN. The results of an experiment carried out with nitrodurene in ACN in the presence of 2% H_2O are also given. Electron transfer is then slower than for ACN without added water, emphasising the specific solvation of the anion radical by water molecules.

In all cases, the plots of $\log k(E)$ against E appear as bent toward the potential axis, indicating a dependence of the apparent transfer coefficient on the potential. This is better seen on the plots of α_{ap} against E [fig. 2(b)] obtained by differentiation of the $\log k(E)$ against E curves [eqn (1)]. The apparent transfer coefficient thus appears as an approximately linear function of the electrode potential. However, we should ask whether this reflects an actual variation of the true transfer coefficient or a double-layer effect deriving from the variation of φ_r with the electrode potential. Differentiation of eqn (2) leads to:

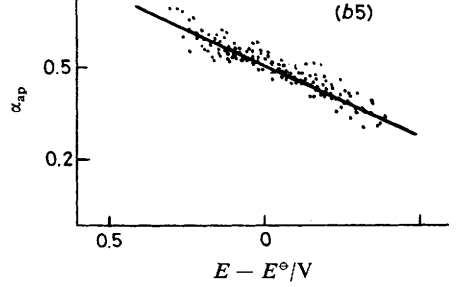
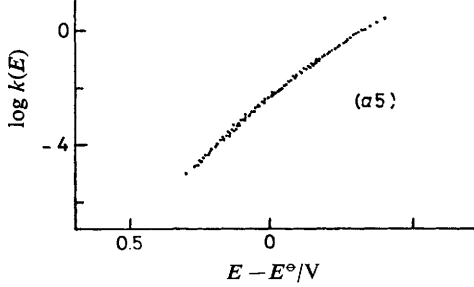
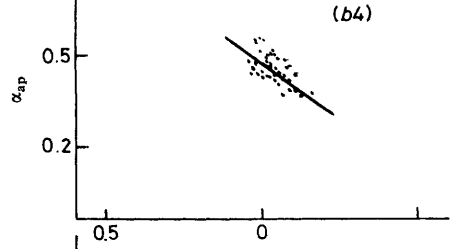
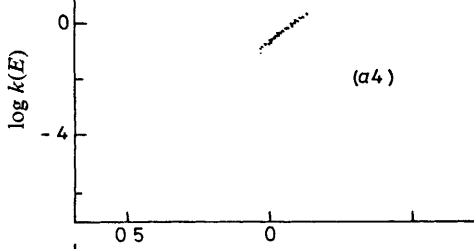
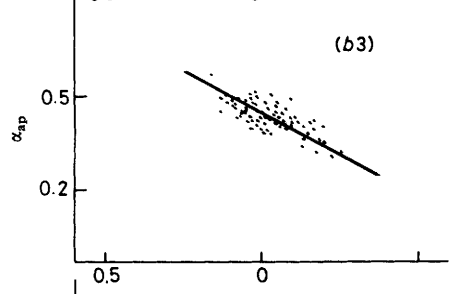
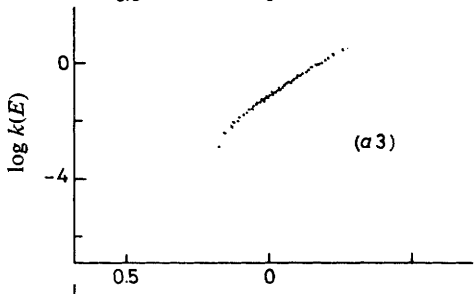
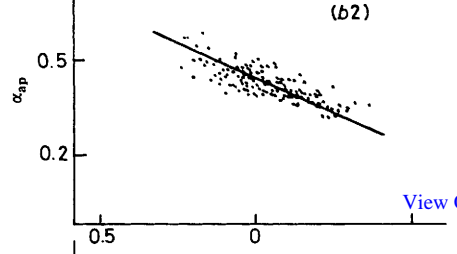
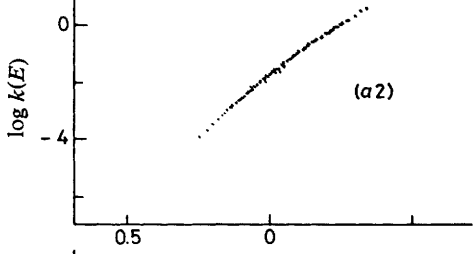
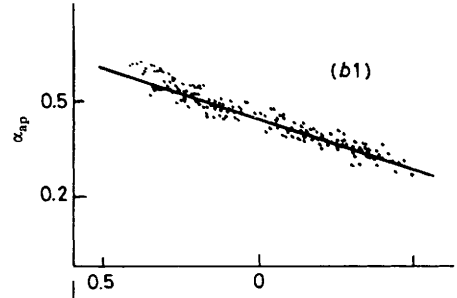
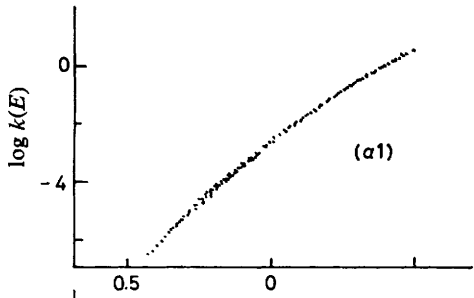
$$\frac{\partial \bar{\alpha}}{\partial E} = \frac{1}{1 - \frac{\partial \varphi_r}{\partial E}} \frac{\partial \alpha_{ap}}{\partial E} + \frac{1}{\left(1 - \frac{\partial \varphi_r}{\partial E}\right)^2} \alpha_{ap} \frac{\partial^2 \varphi_r}{\partial E^2}. \quad (4)$$

Fig. 3 shows the variations of φ_2 , the potential difference between the outer Helmholtz plane and the solution, and of $\partial \varphi_2 / \partial E$ and $\partial^2 \varphi_2 / \partial E^2$ with the electrode potential. If we assume that the reaction site is located at the o.H.p. it is seen that in the pertinent potential ranges $\partial^2 \varphi_2 / \partial E^2$ is so small that the second term in eqn (4) is negligible in comparison with the first. Even if the reaction site is closer to the electrode surface as it indeed appears to be (by ca. 20% in the case of the considered molecules with NBu_4^+ as supporting cation),²⁶ the above estimation will not be significantly altered.

A first conclusion is that the electrochemical transfer coefficient does vary with potential beyond experimental error for the reactions considered. It is then of interest to compare the observed variation with that predicted by the Marcus theory. This is shown in table 1. k_s and hence λ_0 were estimated on the basis of two different assumptions. In the first of these φ_r is taken as equal to zero and in the second $\varphi_r = \varphi_2$, i.e. the reaction site is regarded as located at the o.H.p. With both assumptions it is observed that the experimental and predicted variations of the transfer coefficient with potential are of the same order of magnitude. Location of the reaction site closer to the electrode surface²⁶ would obviously not significantly alter this conclusion.

Note that electron transfer to the same compound, t-nitrobutane, is faster in DMF than in ACN. This reflects the stronger solvating power of the latter toward anions or, alternatively, the greater availability of residual water, a specific solvation agent, in ACN than in DMF. In both cases this is in agreement with ACN being a stronger acid and a weaker base (in a broad sense) than DMF.

On the other hand, note that the value of $\alpha(E^\ominus + \varphi_2)$ is smaller than predicted by the Marcus theory (0.5), the difference being more important in ACN than in DMF.



[View Online](#)

A possible explanation of this phenomenon is that the solvation mode is different in the starting molecule and in the anion radical especially as far as preferential solvation by water is concerned. In the framework of an harmonic approximation the parabola representing the potential energy of the product as a function of the reaction coordinate would then be tighter than that corresponding to the reactant.

IMPEDANCE MEASUREMENTS

The reduction of nitromesitylene in ACN [fig. 2(a), table 1] illustrates the limitation of the c.p.s.v. technique. For this relatively fast electron transfer, $k_{s,ap} = 0.2 \text{ cm s}^{-1}$, reasonably accurate kinetic data could only be obtained in a narrow range of sweep rate and thus a narrow range of potentials. In order to overcome these difficulties the impedance method was used with the aim of investigating this even faster electron-transfer processes. The measurement technique we used was basically the same as already described²² involving the use of a two-electrode configuration and of a lock-in amplifier providing the in-phase and quadrature component of the first harmonic current response to a small (5 mV amplitude) sinusoidal input voltage. Since we wished to investigate fast electron transfers, frequencies up to 20 kHz were used. Special care is then required to extract the faradaic resistance and capacitance from the overall output signal. On the other hand, the measurements have to be carried out for a large number of values of the d.c. potential since we are looking for small variations of α . These are the two reasons why the in-phase and quadrature component were digitized and then stored and treated in an on-line computer. A detailed description of the instrumentation and procedures used is given elsewhere.²⁷

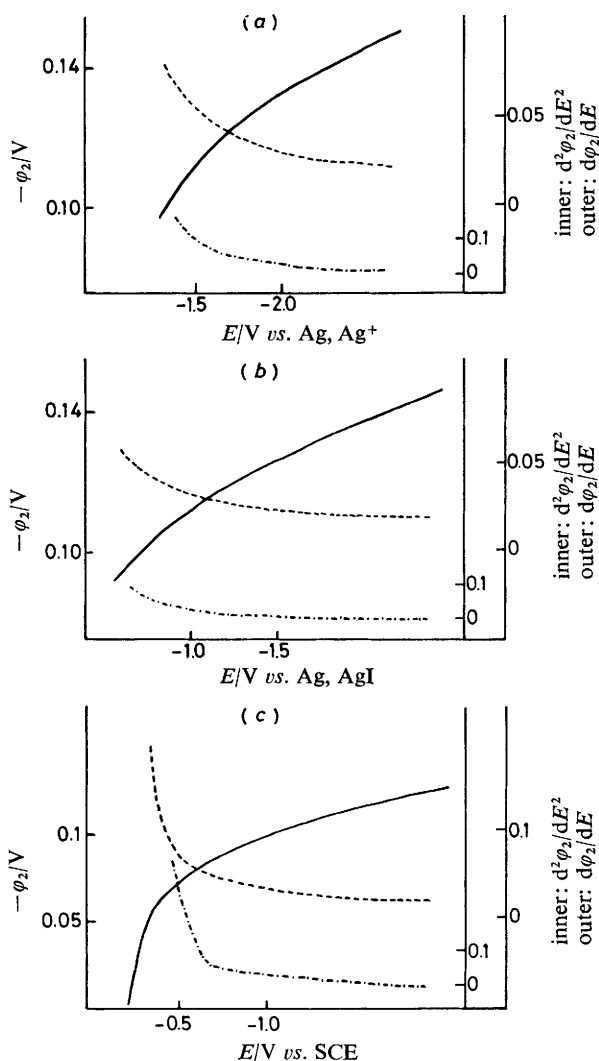
The potential-dependent charge-transfer rate constant was derived from the faradaic resistance, R_f , and capacitance, C_f , according to:²⁷

$$\log k(E) = \log(D_A^\ddagger) - \log \frac{(R_f C_f \omega - 1) \left[1 + \exp\left(\frac{F}{RT}(E - E_{\frac{1}{2}})\right) \right]}{(2\omega)^\ddagger}$$

where ω is the pulsation of the input signal, E the d.c. potential and $E_{\frac{1}{2}}$ the reversible half-wave potential. D_A^\ddagger and $E_{\frac{1}{2}}$ were derived from the height and location, respec-

FIG. 2.—(a) Forward charge-transfer rate constant in ACN and DMF with $0.1 \text{ mol dm}^{-3} \text{ Bu}_4\text{NI}$ as a function of the electrode potential as obtained from c.p.s.v. (b) Variation of the apparent transfer coefficient with potential. (1) 3.0 mmol dm^{-3} t-nitrobutane in ACN; (2) 2.0 mmol dm^{-3} nitroindurene in ACN + 2% H_2O ; (3) 2.1 mmol dm^{-3} nitroindurene in ACN; (4) $1.64 \text{ mmol dm}^{-3}$ nitromesitylene in ACN; (5) 2.5 mmol dm^{-3} t-nitrobutane in DMF. The various points were obtained with the following sweep rate (V s^{-1})

system	cathodic scan								
1	2166	724	216	72.2	23.6	6.60	2.40	0.75	0.15
2	2194	707	228	66.1	22.6	6.55	2.42	0.65	0.25
3	2322	651	221	69.4	23.5	6.96	2.31		
4		659	238	65.1	23.6	6.56			
5	2165	750	218	71.3	22.9	6.95	2.39	0.70	0.24
system	anodic scan								
1	2161	669	212	67.7	22.1	6.96	2.34	0.77	0.14
2	2076	596	205	56.1	20.4	6.41	2.10	0.64	0.21
3	2227	722	218	69.4					
4									
5	2171	729	208	68.8	21.9	6.70	2.30		



View Online

FIG. 3.—Potential difference between the o.H.p. (—) and the solution and its first (---) and second (— · —) derivatives. (a) ACN + 0.1 mol dm⁻³ Bu₄NI; (b) DMF + 0.1 mol dm⁻³ Bu₄NI; (c) EtOH + 0.4% H₂O + 1 mol dm⁻³ Bu₄NI + 0.012 mol dm⁻³ Bu₄NOH.

tively, of the minimum of the faradaic capacitance as a function of the d.c. potential:

$$\frac{1}{C_f \omega} = \frac{4RT}{F^2 SC^0 (2\omega D_A)^{\frac{1}{2}}} \cosh^2 \left(\frac{F}{2RT} (E - E_{\frac{1}{2}}) \right)$$

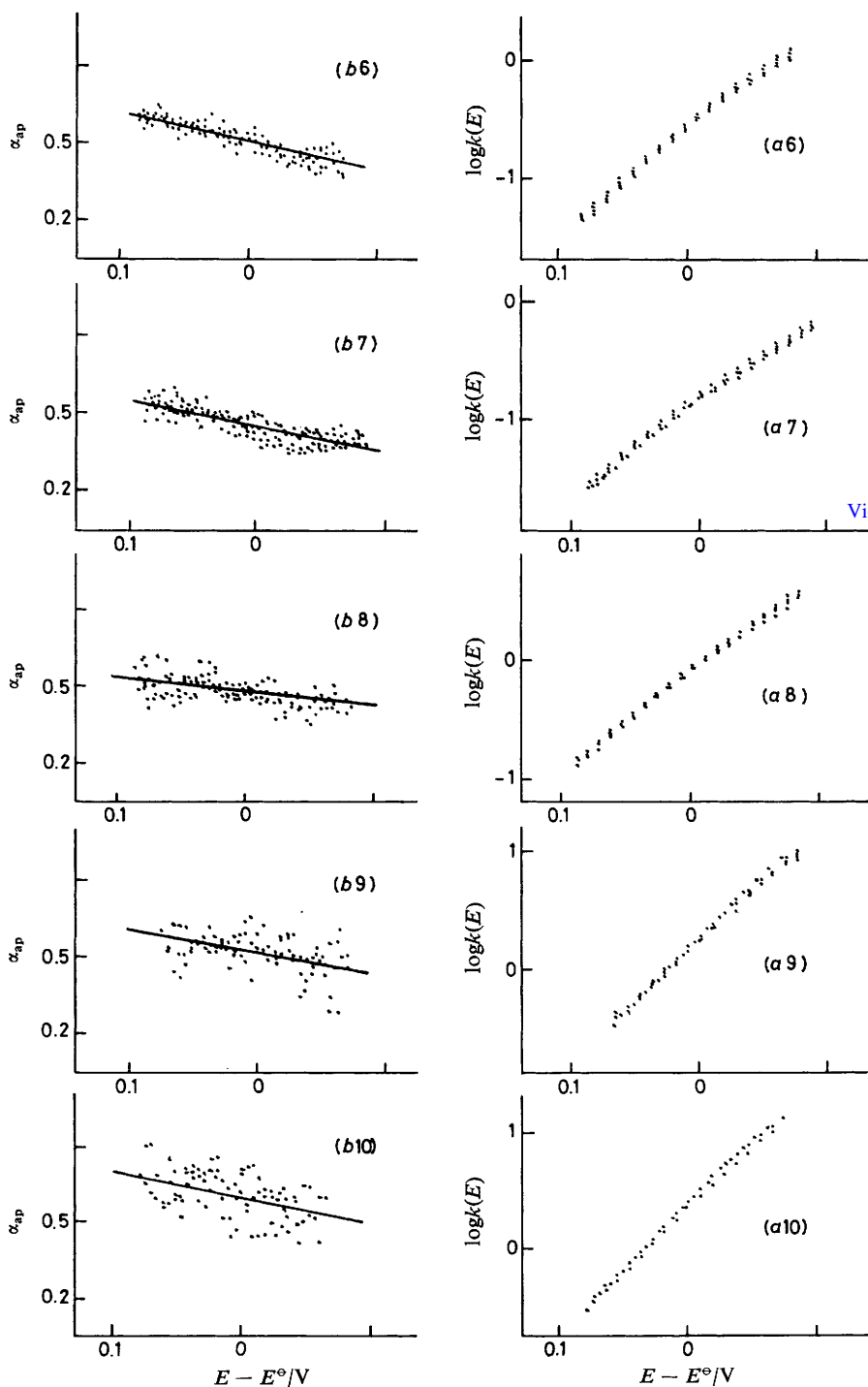
where C^0 is the initial concentration of A.

Fig. 4(a) shows plots of $\log k(E)$ against E obtained for nitromesitylene, nitrodurene, terephthalonitrile, phthalonitrile and *p*-diacetylbenzene in DMF. Differentiation of these curves gives the variation of the apparent transfer coefficient with the potential. An approximate linear dependence is again observed [fig. 4(b)]. While this is clearly the case for the first three compounds, the results obtained with phthalonitrile and *p*-diacetylbenzene show less accuracy, corresponding to the fact that these

TABLE 1.—PREDICTED AND OBSERVED VARIATION OF ELECTROCHEMICAL TRANSFER COEFFICIENT

solvent	reactant	$-E^{\circ a}$ /V	D_A /cm ² s ⁻¹	Z_{el} /cm s ⁻¹	$(\partial \alpha_0 / \partial E)$ /V ⁻¹	k_s /cm s ⁻¹	$\phi_r = 0$			$\phi_r = \phi_2$			
							(λ_0/F) /V	$\alpha(E^{\circ})$ +	$(\partial \alpha / \partial E)$ /V ⁻¹	(λ_0/F) /V	$\alpha(E^{\circ})$ +	$(\partial \alpha / \partial E)$ /V ⁻¹	
ACN	t-nitrobutane	1.998	3.0×10^{-5}	6200	0.33 (± 0.01)	2.0 (± 0.2) $\times 10^{-3}$	1.52 (± 0.01)	0.44 (± 0.006)	0.165 (± 0.002)	1.9 (± 0.2) $\times 10^{-2}$	1.29 (± 0.01)	0.41 (± 0.006)	0.174 (± 0.002)
DMF	t-nitrobutane	1.277	1.3×10^{-5}	6200	0.48 (± 0.03)	4.8 (± 1.0) $\times 10^{-3}$	1.43 (± 0.03)	0.51 (± 0.015)	0.240 (± 0.003)	5.0 (± 1.1) $\times 10^{-2}$	1.19 (± 0.03)	0.46 (± 0.016)	0.210 (± 0.004)
ACN + 2% H ₂ O	nitrodiurene	1.619	1.9×10^{-5}	4700	0.45 (± 0.04)	1.6 (± 0.1) $\times 10^{-2}$	1.28 (± 0.01)	0.44 (± 0.018)	0.225 (± 0.002)	1.2 (± 0.1) $\times 10^{-1}$	1.08 (± 0.01)	0.40 (± 0.020)	0.23 (± 0.002)
ACN	nitrodiurene	1.714	1.9×10^{-5}	4700	0.55 (± 0.06)	6.0 (± 0.5) $\times 10^{-2}$	1.15 (± 0.01)	0.45 (± 0.031)	0.275 (± 0.002)	4.7 (± 0.4) $\times 10^{-1}$	0.94 (± 0.01)	0.40 (± 0.033)	0.267 (± 0.003)
ACN	nitromesitylene	1.667	1.9×10^{-5}	4900	0.75 (± 0.10)	2.0 (± 0.1) $\times 10^{-1}$	1.03 (± 0.01)	0.48 (± 0.05)	0.37 (± 0.001)	1.64 (± 0.06)	0.81 (± 0.01)	0.40 (± 0.08)	0.307 (± 0.002)

^a E is referred to the Ag/Ag⁺ electrode in ACN, and to the Ag/AgI electrode in DMF.



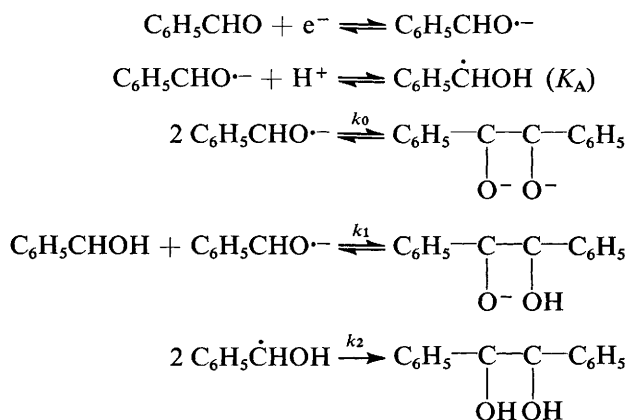
compounds give rise to very fast charge transfer (table 2). The variations of φ_2 with potential [fig. 3(b)] are again too small to be responsible for the variation of the apparent transfer coefficient with potential. In fact, they can again be neglected when passing from the variation of the apparent transfer coefficient to the variation of the intrinsic transfer coefficient [eqn (4)].

Comparison of the experimental and predicted potential dependence of the transfer coefficient was made in the same way as in the preceding section. The results (table 2) show that the experimental and predicted variations are again of the same order of magnitude.

REACTIONS INVOLVING CHEMICAL STEPS COUPLED WITH THE ELECTRON-TRANSFER PROCESS

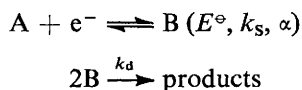
REDUCTION OF BENZALDEHYDE IN ALKALINE ETHANOL

The reduction of benzaldehyde in alkaline ethanol or water + ethanol mixtures has been shown to involve dimerization reactions following the initial charge-transfer step.²⁸⁻³⁰ Since the apparent rate of dimerization increases with decreasing pH, the reduction mechanism is likely to involve the following steps:



[View Online](#)

Since the mono- and di-pinacolate are rapidly protonated in the considered pH range (15.5-17) and since the protonation of the anion radical is fast and reversible, the overall reaction scheme is equivalent to:



with k_d the apparent dimerization rate constant.

The kinetic control of the overall reaction depends upon two parameters featuring the rate of the electron transfer and the rate of the dimerization reaction relative to the rate of diffusion. In cyclic voltammetry and convolution potential-sweep voltam-

FIG. 4.—(a) Forward charge-transfer rate constant as a function of the electrode potential as obtained for impedance measurements. (b) Variation of the apparent transfer coefficient with potential. Solvent: DMF; supporting electrolyte: 0.5 mmol dm⁻³ NBu₄I. (6) 0.76 mmol dm⁻³ nitromesitylene; (7) 1.0 mmol dm⁻³ nitroindurene; (8) 0.95 mmol dm⁻³ terephthalonitrile; (9) 0.94 mmol dm⁻³ phthalonitrile; (10) 1.0 mmol dm⁻³ *p*-diacetylbenzene. The various points were obtained with the following frequencies (kHz): 1, 2.5, 5, 10, 20 for (6) and (7); 2.5, 5, 10, 20 for (8)-(10).

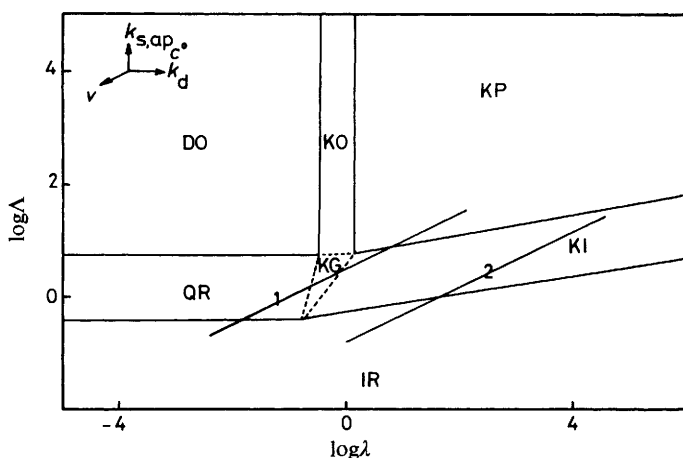
TABLE 2.—CHARACTERISTICS OF THE CHARGE-TRANSFER KINETICS AND COMPARISON WITH THE MARCUS THEORY

reactant	$-E^\circ$ /V vs. SCE	D_A $/10^{-6}$ cm^2 s^{-1}	Z_{ei} $/\text{cm}$ s^{-1}	$(\partial\alpha_{ap}/\partial E)$ $/\text{V}^{-1}$	ϕ_r	$k_s/\text{cm s}^{-1}$	$(\lambda_0/F)/\text{V}$	$\alpha(E^\circ + \phi_r)$	$(\partial\alpha/\partial E)/\text{V}^{-1}$	
									Marcus	exptl
nitroarene	1.390	6.2	4700	0.98 ± 0.09	0	0.15 ± 0.01	1.05 ± 0.01	0.45	0.238 ± 0.002	0.49 ± 0.05
nitromesitylene	1.351	9.5	4900	1.09 ± 0.10	ϕ_2	0.82 ± 0.04	0.88 ± 0.01	0.36	0.284 ± 0.002	
terephthalonitrile	1.482	9.2	5500	0.56 ± 0.09	ϕ_2	0.29 ± 0.01	0.99 ± 0.01	0.51	0.253 ± 0.002	0.54 ± 0.05
phthalonitrile	1.560	9.0	5500	0.88 ± 0.18	0	1.85 ± 0.05	0.80 ± 0.01	0.41	0.312 ± 0.002	
<i>p</i> -diacetylbenzene	1.389	6.9	4900	1.0 ± 0.2	ϕ_2	0.82 ± 0.03	0.90 ± 0.01	0.48	0.279 ± 0.002	0.28 ± 0.05
						5.55 ± 0.20	0.70 ± 0.01	0.43	0.357 ± 0.002	
						2.00 ± 0.05	0.81 ± 0.02	0.62	0.311 ± 0.003	0.44 ± 0.09
						23.5 ± 0.6	0.55 ± 0.02	0.54	0.451 ± 0.003	
						2.30 ± 0.12	0.78 ± 0.02	0.60	0.321 ± 0.003	0.50 ± 0.10
						22.3 ± 1.2	0.55 ± 0.02	0.51	0.456 ± 0.003	

metry, which is the technique we used for investigating this reaction, the two parameters are conveniently expressed as:

$$\Lambda = k_{s,ap} \left(\frac{RT}{D_A F v} \right)^{\frac{1}{2}} \text{ and } \lambda = \frac{RT}{F} \frac{k_d C^{\circ}}{v}$$

where C° is the initial concentration of A. A semi-quantitative representation of how the kinetic control varies with Λ and λ is shown in fig. 5.³¹ In this representation the potential dependence of the transfer coefficient is neglected and α is taken as equal to 0.5. This does not correspond to the actual characteristics of the reaction we are investigating. However, it is sufficient for defining the various kinetic zones and the



View Online

FIG. 5.—Kinetic zone diagram for an irreversible dimerization following the charge-transfer process. The two oblique segments (1) and (2) show the shift of the system when varying the sweep rate from 0.07 to 2330 V s⁻¹ for pH 17 and 15.5, respectively.

nature of the kinetic control. DO corresponds to diffusion-controlled Nernstian behaviours, QR and IR to quasi-reversible and totally irreversible kinetic control by charge transfer, KP to “pure kinetic” control by the dimerization reaction and KO to mixed diffusion-kinetic control involving the dimerization reaction with no interference from the charge-transfer kinetics in the two latter cases. KI still corresponds to “pure kinetic” conditions with regard to the dimerization reaction, *i.e.* to mutual compensation between diffusion and the chemical reaction. Kinetic control by charge transfer, however, interferes concomitantly. KG represents the general case. Information about the kinetics of the electron-transfer steps can be obtained as long as the system is in a kinetic situation corresponding to the QR, IR or KI zones. For QR, the potential-dependent forward rate constant can be derived from the kinetic data in the same manner as in the absence of follow-up reaction, *i.e.* according to eqn (3). In the IR case, this relationship simplifies into:

$$\log(k)E = \log(D_A^{\ddagger}) - \log \frac{I_1 - I}{i}$$

In the KI zone, $k(E)$ can still be obtained using a different expression:

$$\log k(E) = \log(D_A^{\ddagger}) - \log \frac{I_1 - I - i^{\frac{1}{2}} \exp \left[\left(\frac{F}{RT} \right) (E - E_k) \right]}{i} \tag{5}$$

with

$$E_k = E^\ominus + \frac{RT}{3F} \ln \frac{2k_d C^\ominus}{3I_1} \quad (6)$$

E_k can be obtained as soon as the system enters the KP zone. Then:

$$E = E_k + \frac{RT}{F} \ln \frac{I_1 - I}{i^{\frac{1}{3}}} \quad (7)$$

At pH 17 (0.012 mol dm⁻³ Bu₄NOH + 1 mol dm⁻³ Bu₄NI), the system lies in the KP zone at low sweep rates (0.07, 0.22 and 0.68 V s⁻¹). The corresponding log analysis [eqn (7)] gives rise to a straight line with the correct slope (59 ± 1 mV). The potential location of the straight line provides the value of E_k , -1.451 V vs. SCE. At high sweep rates (69, 227, 700 and 2330 V s⁻¹) the system is shifted into the QR zone. The standard potential can then be determined as $E_d = -1.615$ V. From eqn (6) it follows that $k_d = (3.3 \pm 1.5) 10^5$ dm³ mol⁻¹ s⁻¹. On the other hand, application of eqn (3) provides the potential-dependent forward electron-transfer rate constant $k(E)$ in the high-sweep-rate region [fig. 6(a)] and, by differentiation, the variations of the apparent transfer coefficient with potential [fig. 6(b)].

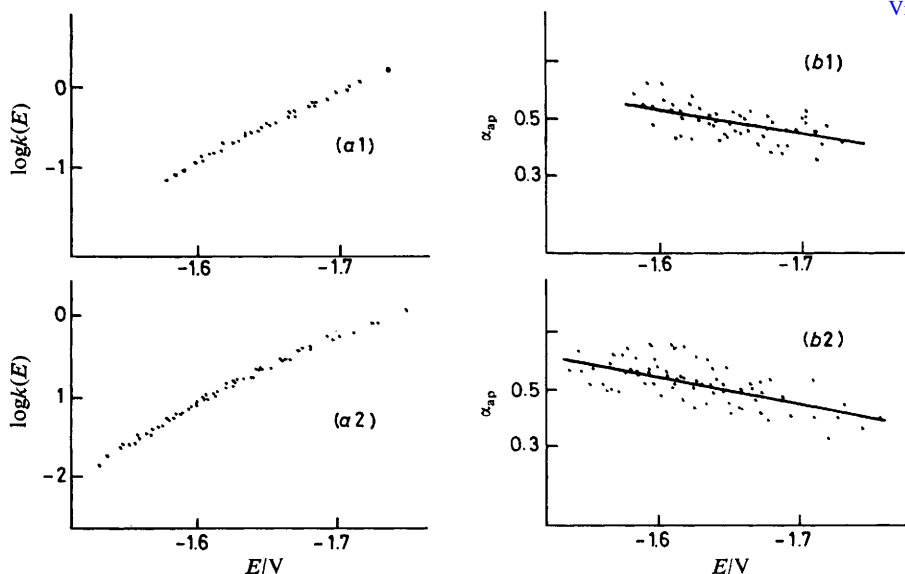


FIG. 6.—Reduction of benzaldehyde in ethanol. (a) Forward electron-transfer rate constant as a function of the electrode potential (from c.p.s.v. data); (b) variation of the apparent transfer coefficient with potential. (1) pH = 17, $v = 69, 227, 700$ and 2330 V s⁻¹; (2) pH = 15.5, $v = 0.22, 0.69, 2.27, 6.8, 22.4, 69, 222, 689$ and 2200 V s⁻¹.

At pH 15.5 (phenol buffer), the system lies in the KI zone in almost all the available sweep-rate range. The KP zone is reached only for the slowest sweep rate (0.07 V s⁻¹) which gives access to E_k , $E_k = -1.413$ V. We thus found that $k_d = (5 \pm 3) \times 10^7$ dm³ mol⁻¹ s⁻¹, taking for E^\ominus the same value as at pH 17. This confirms the increase of the apparent dimerization rate constant upon decreasing the pH. In the KI zone, the treatment of data through eqn (5) taking into account the above value of E_k provides $k(E)$ [fig. 6(a)] and, by differentiation, α_{ap} [fig. 6(b)].

At both pH α_{ap} appears as an approximately linear function of potential. Again

the variations of the o.H.p. potential ϕ_2 with the electrode potential [fig. 3(c)] are too small to be responsible for the variation of α_{ap} . Comparison with the Marcus theory is shown in table 3, along the same lines as in the preceding sections.

TABLE 3.—COMPARISON OF PREDICTED AND OBSERVED ELECTROCHEMICAL TRANSFER COEFFICIENT

pH	$-E^\ominus$ /V vs. SCE	D^A /10 ⁻⁶ cm ² s ⁻¹	Z_{e1} /cm s ⁻¹	$(\partial\alpha_{ap}$ / ∂E) /V ⁻¹	ϕ_r	k_s /cm s ⁻¹	(λ_0/F) /V	$\alpha(E^\ominus$ + $\phi_r)$	$(\partial\alpha/\partial E)/V^{-1}$	
									Marcus	exptl
17	1.615	6.3	6070	0.85	0	0.17	1.07	0.52	0.24	0.42
					ϕ_2	1.5	0.84	0.43	0.30	0.44
15.5	1.615	6.3	6070	0.94	0	0.12	1.10	0.54	0.23	0.47
					ϕ_2	1.2	0.87	0.43	0.29	0.48

CONCLUDING REMARKS

For all the organic systems investigated in this study there is a definite tendency for the electrochemical transfer coefficient to vary with the electrode potential whether the investigation was carried out by convolution potential-sweep voltammetry or by the impedance method. This was shown to occur for a series of simple electron-transfer reactions but could also be detected for a more complex reaction involving a chemical reaction following the initial electron-transfer process. In all cases, the variations of the potential at the reaction site with the electrode potential were too small to be considered as responsible for the observed variation. It is thus concluded that the actual transfer coefficient does vary with the electrode potential. Correlating the observed potential dependence with the reorganization factor according to the Marcus theory, it was observed that the experimental and predicted variations are of the same order of magnitude. In most cases the agreement is not quantitative. The concordance between theory and experimental data can, however, be considered as satisfactory taking into account the crudeness of the Marcus model. Rather than an unexpected quantitative agreement, the important point is that the variations of the electrochemical transfer coefficient are experimentally significant, indicating a definite curvature of the potential-energy surfaces of the same order of magnitude as predicted by the theory. It is interesting to note that, although the rate data depend upon electrode pre-treatment, the variations of α found for t-nitrobutane on platinum are of the same order of magnitude as those found on mercury.¹⁸

These results contrast with those found for the reduction of chromium complexes in water, for which the possible variations of α have been very thoroughly and critically investigated.¹³ In these cases, no potential dependence of the transfer coefficient was detected, at least in potential ranges cathodic to the standard potential. Experimental precision and extension of the explored potential range were sufficient for leaving little doubt that if a variation of α of the order of magnitude predicted by the Marcus theory had occurred it would have been detected. More recent investigations¹⁹ revealed that for the aquo Cr³⁺/Cr²⁺ system variations of α with potential exist on the anodic side while they do not on the cathodic side, but are much larger than predicted for an outer-sphere electron transfer. In the case of the above organic systems it is worth emphasizing that the variations of α are the same in the potential regions either negative or positive to the standard potential. The outer-sphere character of the electron-transfer process in the case of the chromium complexes is not evident.

Electron transfer is very slow (k_s is of the order of 10^{-6} cm s $^{-1}$), implying considerable re-organization in the inner coordination sphere. The above organic reactions involving fast electron transfer meet the requirements of an outer-sphere process. They most probably involve small changes in bond distances and angles, solvation being the main reorganization factor.

We thank Dr D. Garreau for his helpful collaboration in the impedance determinations. This work was supported in part by the C.N.R.S. (ERA 309 "Electrochimie Moléculaire").

- ¹ P. P. Schmidt, *Electrochemistry* (Specialist Periodical Report, The Chemical Society, London, 1974), vol. 5, p. 21.
- ² R. A. Marcus, *J. Chem. Phys.*, 1965, **43**, 679.
- ³ R. A. Marcus, in *Dalhem Workshop on the Nature of Sea Water*, Dahlem Konferenzen, ed. E. D. Goldberg (Abakon Verlagsgesellschaft, West Berlin, 1975), pp. 447-504.
- ⁴ N. S. Hush, *J. Chem. Phys.*, 1958, **28**, 962.
- ⁵ R. Parsons and E. Passeron, *J. Electroanal. Chem.*, 1966, **12**, 525.
- ⁶ D. M. Mohilner, *J. Phys. Chem.*, 1969, **73**, 2652.
- ⁷ F. C. Anson, N. Rathjen and R. D. Frisbee, *J. Electrochem. Soc.*, 1970, **117**, 477.
- ⁸ D. H. Angell and T. Dickinson, *J. Electroanal. Chem.*, 1972, **35**, 55.
- ⁹ K. Suga, H. Mizota, Y. Kanzaki and S. Aoyagni, *J. Electroanal. Chem.*, 1973, **41**, 313.
- ¹⁰ E. Momot and G. Bronoel, *C.R. Acad. Sci.*, 1974, **278**, 319.
- ¹¹ P. Bindra, A. P. Brown, M. Fleischmann and D. Pletcher, *J. Electroanal. Chem.*, 1975, **58**, 39.
- ¹² J-M. Savéant and D. Tessier, *J. Electroanal. Chem.*, 1975, **65**, 57.
- ¹³ M. J. Weaver and F. C. Anson, *J. Phys. Chem.*, 1976, **80**, 1861.
- ¹⁴ Z. Samec and J. Weber, *J. Electroanal. Chem.*, 1977, **77**, 163.
- ¹⁵ J-M. Savéant and D. Tessier, *J. Phys. Chem.*, 1977, **81**, 2192.
- ¹⁶ J-M. Savéant and D. Tessier, *J. Phys. Chem.*, 1978, **82**, 1723.
- ¹⁷ D. Garreau, J-M. Saveant and D. Tessier, *J. Phys. Chem.*, 1979, **83**, 3003.
- ¹⁸ D. A. Corrigan and D. H. Evans, *J. Electroanal. Chem.*, 1980, **106**, 287.
- ¹⁹ P. D. Tyma and M. J. Weaver, *J. Electroanal. Chem.*, 1980, **111**, 195.
- ²⁰ W. R. Fawcett and R. O. Loufty, *Can. J. Chem.*, 1973, **51**, 230.
- ²¹ W. R. Fawcett, B. M. Ikeda and J. B. Sellan, *Can. J. Chem.*, 1979, **57**, 2268.
- ²² H. Kojima and A. J. Bard, *J. Am. Chem. Soc.*, 1975, **97**, 6317.
- ²³ M. E. Peover and J. S. Powell, *J. Electroanal. Chem.*, 1969, **20**, 427.
- ²⁴ J. C. Imbeaux and J-M. Savéant, *J. Electroanal. Chem.*, 1973, **44**, 169.
- ²⁵ J-M. Savéant and D. Tessier, *J. Electroanal. Chem.*, 1975, **62**, 57.
- ²⁶ J-M. Savéant and D. Tessier, to be submitted.
- ²⁷ D. Garreau, J-M. Savéant and D. Tessier, *J. Electroanal. Chem.*, 1979, **103**, 321.
- ²⁸ L. Nadjo and J-M. Savéant, *J. Electroanal. Chem.*, 1971, **33**, 419.
- ²⁹ F. Ammar, L. Nadjo and J-M. Savéant, *J. Electroanal. Chem.*, 1973, **47**, 146.
- ³⁰ J. W. Hayes, I. Ruzic and D. E. Smith, *J. Electroanal. Chem.*, 1974, **51**, 269.
- ³¹ L. Nadjo and J-M. Savéant, *J. Electroanal. Chem.*, 1973, **48**, 113.